

Lawrence Berkeley National Laboratory

LBL Publications

Title

Mass spectrometry imaging—based assays for aminotransferase activity reveal a broad substrate spectrum for a previously uncharacterized enzyme

Permalink

<https://escholarship.org/uc/item/9w38s6hc>

Journal

Journal of Biological Chemistry, 299(3)

ISSN

0021-9258

Authors

de Raad, Markus

Koper, Kaan

Deng, Kai

et al.

Publication Date

2023-03-01

DOI

10.1016/j.jbc.2023.102939




Peer reviewed



Mass spectrometry imaging–based assays for aminotransferase activity reveal a broad substrate spectrum for a previously uncharacterized enzyme

Received for publication, September 27, 2022, and in revised form, January 19, 2023. Published, Papers in Press, January 24, 2023.

<https://doi.org/10.1016/j.jbc.2023.102939>

Markus de Raad^{1,*}, Kaan Koper², Kai Deng^{3,4}, Benjamin P. Bowen^{1,5}, Hiroshi A. Maeda², and Trent R. Northen^{1,3,5}

From the ¹Environmental Genomics and Systems Biology Division, Lawrence Berkeley National Laboratory, Berkeley, California, USA; ²Department of Botany, University of Wisconsin-Madison; Madison, Wisconsin, USA; ³Joint BioEnergy Institute, Lawrence Berkeley National Laboratory, Emeryville, California, USA; ⁴Sandia National Laboratories, Livermore, California, USA; ⁵Joint Genome Institute, Lawrence Berkeley National Laboratory, Berkeley, California, USA

Reviewed by members of the JBC Editorial Board. Edited by Joseph Jez

Aminotransferases (ATs) catalyze pyridoxal 5'-phosphate–dependent transamination reactions between amino donor and keto acceptor substrates and play central roles in nitrogen metabolism of all organisms. ATs are involved in the biosynthesis and degradation of both proteinogenic and non-proteinogenic amino acids and also carry out a wide variety of functions in photorespiration, detoxification, and secondary metabolism. Despite the importance of ATs, their functionality is poorly understood as only a small fraction of putative ATs, predicted from DNA sequences, are associated with experimental data. Even for characterized ATs, the full spectrum of substrate specificity, among many potential substrates, has not been explored in most cases. This is largely due to the lack of suitable high-throughput assays that can screen for AT activity and specificity at scale. Here we present a new high-throughput platform for screening AT activity using bioconjugate chemistry and mass spectrometry imaging–based analysis. Detection of AT reaction products is achieved by forming an oxime linkage between the ketone groups of transaminated amino donors and a probe molecule that facilitates mass spectrometry-based analysis using nanostructure-initiator mass spectrometry or MALDI–mass spectrometry. As a proof-of-principle, we applied the newly established method and found that a previously uncharacterized *Arabidopsis thaliana* tryptophan AT-related protein 1 is a highly promiscuous enzyme that can utilize 13 amino acid donors and three keto acid acceptors. These results demonstrate that this oxime–mass spectrometry imaging AT assay enables high-throughput discovery and comprehensive characterization of AT enzymes, leading to an accurate understanding of the nitrogen metabolic network.

Aminotransferases (ATs) are a highly versatile class of pyridoxal-5'-phosphate (PLP)-dependent enzymes that transfer an amino group from an amino donor to a keto acceptor substrate *via* the ping-pong bi-bi mechanism (1, 2). ATs are

ubiquitous across all kingdoms of life and are responsible for ~2% of all the reactions that have been assigned an Enzyme Commission number (3, 4). As a result, ATs constitute the largest family of enzymes involved in nitrogen (N) metabolism (Enzyme Commission number 2.6.1.x). For example, in animals, alanine (Ala) ATs play a key role in the Cahill or glucose–Ala cycle, a process occurring in the liver tissue that involves the transamination of Ala to pyruvic acid, which is subsequently converted to glucose *via* gluconeogenesis and transported to muscle tissues for ATP production (5). In gram-negative bacteria, amino sugars found in the lipopolysaccharides present in the outer membrane are usually synthesized from keto-sugars by ATs (6). In plants, the aromatic AT ISS1 regenerates tryptophan using methionine as the amino donor, which connects the biosynthesis of two phytohormones, tryptophan-derived auxin and methionine-derived ethylene (7). Since most ATs transfer an amino group from an amino acid donor to a keto acid acceptor and generate the corresponding keto and amino acid products, AT-catalyzed reactions play pivotal roles in interconnecting different branches of metabolic pathways (8). Thus, an accurate understanding of AT functions is critical for comprehending the architecture and functionality of the N metabolic network, which is currently poorly defined as compared to the carbon metabolic network. This will be highly valuable for a broad range of applications, such as for identifying novel drug targets for cancer therapy, improving plant N use efficiency to enhance crop yield, and optimizing microbial pathways to efficiently produce renewable chemicals and biofuels (9–11).

Notably, many AT enzymes are promiscuous, exhibit broad substrate specificity, and have multiple activities which are likely critical for the plasticity of N metabolic networks (2). For example, yeast aromatic AT 8 is active with aromatic amino acids, methionine, and leucine, while the human kynurenine AT III has both AT and β -lyase activities (2, 12, 13). Despite their importance, however, the full functionalities of ATs, *i.e.*, their substrate specificity profiles, are not well defined. This suggests that there are still many AT-catalyzed reactions that could be physiologically important but are currently unknown.

* For correspondence: Markus de Raad, MdeRaad@lbl.gov.

Mass spectrometry-based screening of aminotransferase

Thus, the large number of AT gene candidates combined with the broad substrate specificity/promiscuity contributed to a low number of fully characterized ATs (2). This large knowledge gap between AT sequence and function is further exacerbated by the lack of suitable high-throughput assays that can screen for AT activity and donor/acceptor specificity.

Conventional AT assays use the intrinsic absorbance or fluorescence of the substrates or reaction products as the readout for AT activity (14). For example, AT assays using tyrosine (Tyr) or α -methylbenzylamine as amino donors measure the absorbance of the deaminated reaction products, 4-hydroxyphenylpyruvic acid and acetophenone, at 331 nm and 245 nm, respectively (15, 16). Alternatively, the reaction products can be derivatized to confer absorbance or fluorescence properties, such as the use of the chromogenic Salkowski reagent to detect the production of indole-3-pyruvic acid (IPA) in tryptophan AT assays (17). Most of these assays can screen multiple AT enzymes using a plate reader but are limited to one specific or a few AT reactions and cannot test incompatible substrate or product pairs. AT activity also can be determined indirectly by coupling the AT reaction with another, more easily detectable, reaction. For example, Ala AT activity can be coupled to the rate of NADH oxidation by lactate dehydrogenase, which forms the basis of commercial enzyme screening kits. Also, a pH-indicator assay using a pH-sensitive dye was developed where AT activity leads to a reduction in the pH through the use of a combined lactate dehydrogenase and glucose dehydrogenase system (18). Another example is the coupling of AT activity to the detection of H₂O₂ generated through amino acid oxidases using pyrogallol red and horseradish peroxidase (19). Similar to conventional assays, these coupled AT assays are limited to a small number of reactions with combinations of compatible reaction products. For example, lactate dehydrogenase and malate dehydrogenase need to be coupled to the reactions of ATs that act on Ala and aspartate (or pyruvate and oxaloacetate). Other assays use unnatural amino donors, where the formed keto acid analogues self-react to form chromogenic products (20). However, this limits the assay to screen only for different keto acceptors, and the AT must be able to use the unnatural amino donor. Direct analysis of AT activity using native substrates and without the need of coupled assays or derivatized reaction products can be performed using HPLC, capillary electrophoresis, circular dichroism, conductometry, or GLC coupled with mass spectroscopy and NMR (21, 22). However, these techniques are time consuming and have a limited throughput.

Nanostructure-initiator mass spectrometry (NIMS) assays are a type of mass spectrometry-based enzyme assays that overcome the above mentioned challenges on limited throughputs and specificities (23). NIMS assays are an established platform for high-throughput enzyme activity determination, in which perfluorous-tagged substrates are desorbed from a perfluorinated nanostructured silicon surface and analyzed in a mass spectrometer (23–27). Alternatively, MALDI or other laser desorption ionization techniques can be used to analyze perfluorous-tagged substrates. The use of

perfluorous tags improves assay sensitivity by conferring favorable mass spectrometry properties to the analyte, and assays can be performed with perfluorous-tagged substrates or reaction products that can be conjugated with a perfluorous tag (28, 29). Here we report a new method to characterize AT substrate specificity based on the oxime NIMS assay (28). The method utilizes a perfluorous alkoxyamine probe that forms an oxime linkage with ketones that are present in any keto acid products after transamination of amino donors (Fig. 1A). Therefore, all potential AT activities can be analyzed in an unbiased manner. This probe can be added to the reaction mixtures after the transamination reactions and affords highly efficient capture of transamination products into the mass-diagnostic tag with subsequent high sensitivity analysis without separation of the reaction products (28). Arraying the reactions onto the NIMS surface using acoustic sample deposition and subsequent analysis by mass spectrometry imaging (MSI) allows for the high-throughput characterization of AT activity and substrate specificity (Fig. 1B) (30, 31).

Here we showed that the oxime-MSI assay can be used to study substrate specificity of ATs in a high-throughput and semi-quantitative manner. We used recombinant three Tyr and tryptophan ATs from *Arabidopsis thaliana* to screen against 31 amino acid donors in combination with three keto acid acceptors. The results confirmed the previously reported broad substrate specificity of the TyrAT (15) and also revealed that the previously uncharacterized tryptophan AT, TAR1, is a highly promiscuous enzyme that can use 13 different amino donors. This new approach has great promise to rapidly improve our understanding of the substrate specificities of ATs with a broad range of combinations of amino donors and keto acceptors.

Results

Establishing the oxime-MSI at assay using previously characterized AtTAT1

Our work is motivated by the need for a scalable methodology that would enable the high-throughput profiling of AT amino donor and keto acceptor specificities. To this end, we incorporated oxime tagging and subsequent MSI analysis using NIMS (28). For a proof-of-principle, we initially screened the detectable activity of the previously characterized *A. thaliana* Tyr AT 1 (*AtTAT1*) against all 20 proteinogenic amino acids and used α -ketoglutarate (α -KG) as keto acceptor. *AtTAT1* was chosen because its substrate specificity has been extensively studied for each substrate one-by-one using a number of established methods (e.g., spectrometric and HPLC-based assays) (15). Here we determine the conversion of these amino donors into their corresponding keto acids, which can be tagged by the NIMS probe (Fig. 1). Activity was identified as samples having a fractional conversion ratio of >0.1 and a ratio of more than 10 standard deviations above the no amino donor control. By calculating these ratios we help control for variation in mass spectrometry desorption/ionization efficiency across the surface (27). The fractional conversion ratio was calculated by dividing the ion intensity for the conjugated

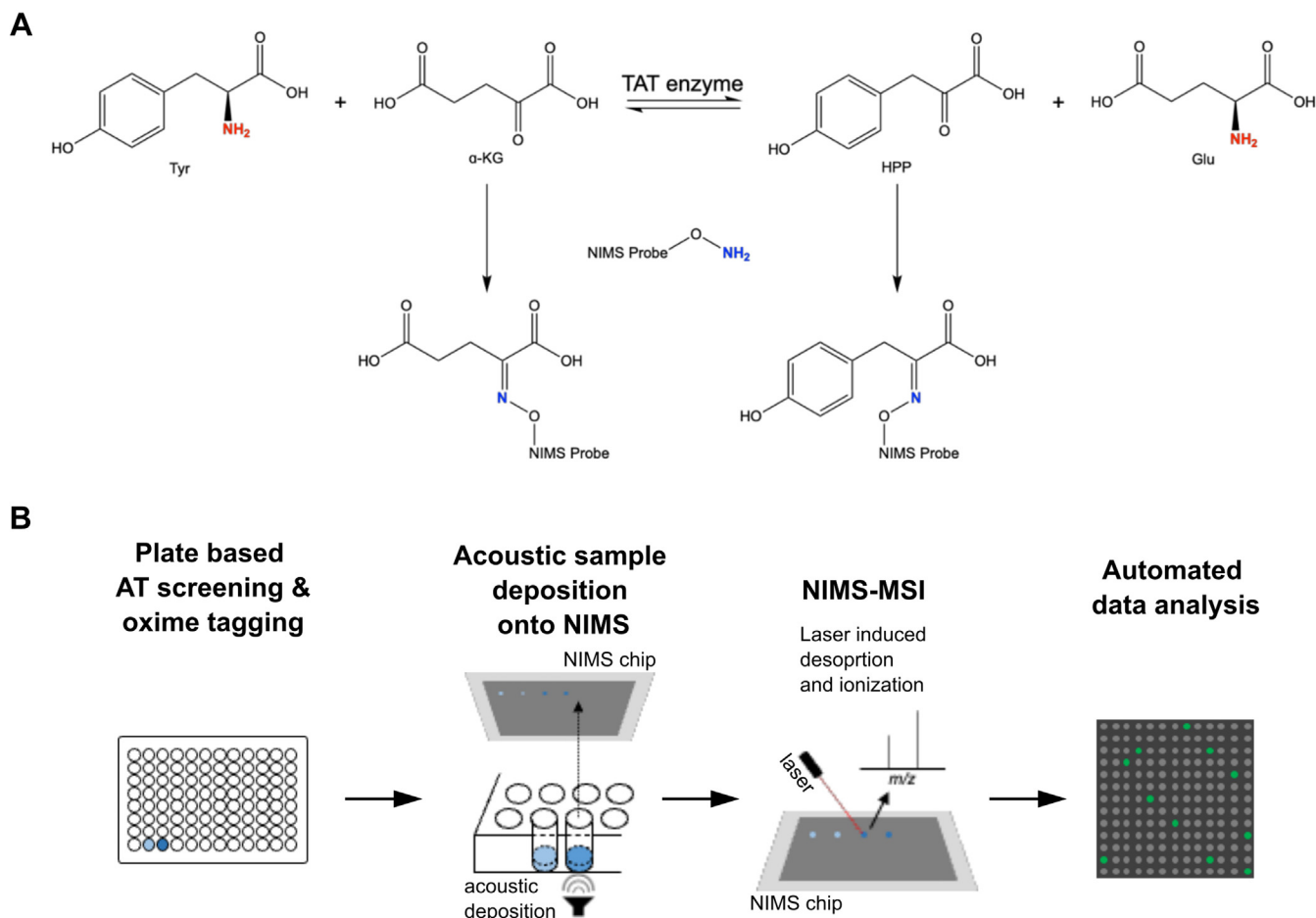


Figure 1. Overview of the oxime-MSI AT assay. A, schematic overview of oxime tagging to detect AT activity. Tyrosine (Tyr) is, for example, transaminated by Tyr AT (TAT) using α -ketoglutarate (α -KG) as keto acceptor yielding 4-hydroxyphenylpyruvate (HPP) and glutamic acid (Glu). The aminoxy group on the oxime probe reacts with the ketone group of α -KG and HPP. The resulting covalent adduct is ready for subsequent MSI analysis. The amino donor involved in the AT reaction is shown in red, while the amine of the NIMS probe is in blue. B, steps in the oxime-MSI AT assay. After the enzymatic reactions and subsequent oxime tagging, samples are printed onto the NIMS surface using acoustic sample deposition. Next, MSI data is acquired and analyzed for AT activity, where positive signals are depicted as green dots. AT, aminotransferase; MSI, mass spectrometry imaging; NIMS, nanostructure-initiator mass spectrometry.

transaminated amino donor by the ion intensity for the conjugated transaminated amino donor plus the ion intensity for conjugated keto acceptor. Historically, we have the authorized ratios of NIMS probe-labeled substrates and products, which is not possible for the oxime-MSI assay (because the oxime probe does not label amino donors). Therefore, an important goal for this initial analysis was to benchmark this approach for enzyme screening against previous reports because media conditions (e.g., pH, ionic strength) may differentially impact the sensitivity of our assay for amino donors *versus* oxime-tagged molecules. Overall, the results from the oxime-MSI AT assays (Fig. 2A) had excellent correlation with those of previous biochemical characterization and showed that *AtTAT1* can use Tyr, histidine (His), leucine (Leu), methionine (Met), phenylalanine (Phe), and tryptophan (Trp) as amino donors in combination with α -KG as a keto acceptor (15). Their keto acid products derived from these amino acid donor substrates were confidently detected after the oxime tagging and MSI (Fig. 2B). The Z-factor, a commonly used statistical measure of the quality of a high-

throughput assay, ranged from 0.76 to 0.92 for all six hits, indicating an excellent assay and suitable for high-throughput screening (HTS) (32). To confirm that the oxime-MSI AT assay can be used in combination with other MSI techniques, activity of *AtTAT1* with Tyr with α -KG as keto acceptor was analyzed with MALDI and yielded the same results as with NIMS (Fig. S2).

Given the potential of the oxime-MSI AT assay to determine amino acceptor preference, we also wanted to test our ability to quantify reaction yields. We expect that the mass spectrometry signal of an oxime-tagged analyte is proportional to all other oxime-tagged analytes, due to the mass spectrometry properties of the probe, and will rise monotonically with its concentration. This allows us to determine the relative preferences of amino donors and keto acceptors based on the ion counts in a semi-quantitative manner. This was confirmed by determining the relative activity of *AtTAT1* with Tyr and α -KG, as lowering the Tyr concentrations resulted in lower fractional conversion ratios for the conversion of Tyr into 4-hydroxyphenylpyruvate (Fig. 2C).

Mass spectrometry-based screening of aminotransferase

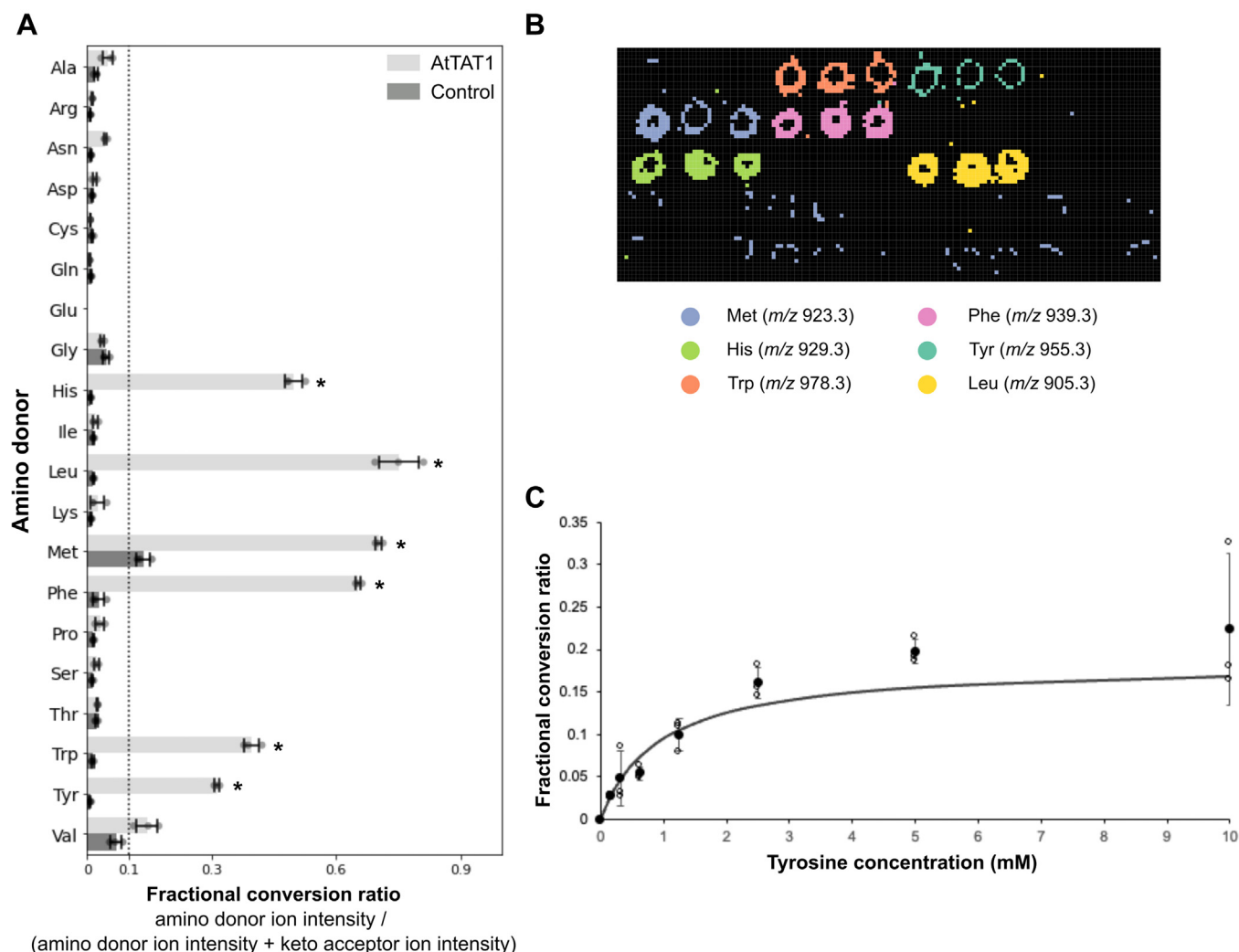


Figure 2. AT amino donor specificity screening using oxime tagging and mass spectrometry analysis. *A*, aminotransferase (AT) activity of *AtTAT1* was analyzed for 20 amino acids using α -KG as a keto acceptor. Bar chart shows the fractional conversion ratios for each amino donor with *AtTAT1* or the control (no amino donor) \pm the standard deviations for three biological replicates. Individual biological replicates are plotted as closed circles. Dotted line indicates a fractional conversion ratio of 0.1. * indicates a fractional conversion ratio of >0.1 and greater than 10 standard deviations compared to the control. *B*, MS image of NIMS surface with printed *AtTAT1* reactions, with the ion intensity visualization of six ions by different false colors representing the oxime probe reacted with transaminated Met, His, Trp, Phe, Tyr, and Leu. *C*, the relative reaction rate of *AtTAT1* with Tyr and α -KG using various concentrations of amino donor tyrosine (0–10 mM). Production of 4-hydroxyphenylpyruvic acid was measured by oxime NIMS. Fractional conversion ratios for the different concentrations of *AtTAT1* are plotted \pm the standard deviations for three biological replicates. Individual biological replicates are plotted as open circles. Solid line represents hyperbolic regression analysis with $y = 0.1705 * x/0.8468 + x$ and $r^2 = 0.67$. *AtTAT1*, *Arabidopsis thaliana* tyrosine aminotransferase 1; Ala, alanine; Arg, arginine; Asn, asparagine; Asp, aspartic acid; Cys, cysteine; Gln, glutamine; Glu, glutamic acid; Gly, glycine; His, histidine; Ile, isoleucine; Leu, leucine; Lys, lysine; Met, methionine; NIMS, nanostructure-initiator mass spectrometry; Phe, phenylalanine; Pro, proline; Ser, serine; Thr, threonine; Trp, tryptophan; Val, valine; α -KG, α -ketoglutarate.

Therefore, our new oxime-MSI AT assay using oxime tagging and subsequent MS analysis was able to accurately determine the substrate specificity of *AtTAT1*.

Characterization of *AtTAR1* against a panel of amino donors and keto acceptors

To further explore the high-throughput potential of the oxime-MSI AT assay, we screened *AtTAT1*, *A. thaliana* tryptophan AT of *Arabidopsis* 1 (*AtTAA1*), and *A. thaliana* tryptophan AT-related protein 1 (*AtTAR1*) for activity against 31 different amino donors using three different keto acid acceptors in a 384-well format using NIMS. The amino donor preference of *AtTAA1* – a tryptophan AT – has previously

been determined and hence included as another control enzyme (33). *AtTAR1* encodes a protein that is 69% identical to *AtTAA1* and is suggested to be a part of the IPA-mediated biosynthetic pathway of the plant hormone auxin (2, 34). The oxime-MSI AT assay used in this study identified that *AtTAR1* can use 13 different amino donors and all three keto acceptors (Fig. 3). *AtTAR1* used the amino acids alanine (Ala), arginine (Arg), asparagine (Asn), aspartic acid (Asp), glutamic acid (Glu), His, Leu, Met, Phe, Trp, and Tyr as well as the non-proteinogenic amino acids 2-aminobutyric acid (AABA), and O-methyl-tyrosine (O-MTY) as amino donors. The specificity of *AtTAR1* for Ala, Glu, Leu, Met, Phe, and Tyr as amino donors by *AtTAA1* was confirmed by the oxime-MSI AT assay (Fig. S3). The only exception was that Trp, a previously

Mass spectrometry-based screening of aminotransferase

confirmed amino donor of *AtTAA1*, was slightly below the activity threshold. Additionally, *AtTAA1* was able to use AABA, Asn, Glu, His, and O-MTY as its amino donors. In terms of their keto acid acceptor specificity, both *AtTAR1* and *AtTAA1*, preferred pyruvate and α -ketoglutarate over phenylpyruvate. Overall, these results demonstrate that the amino donor specificity and keto acceptor preferences of *AtTAR1* are similar to those of *AtTAA1*, except that *AtTAR1* was also able

to use Arg and Asp as amino donors. The oxime-MSI AT assay also confirmed previously known substrates of *AtTAT1* and further revealed its ability to use AABA and O-MTY as amino donors (Fig. S4).

To validate the amino donor specificities identified by the oxime-MSI AT, kinetic parameters of *AtTAA1* and *AtTAR1* against aromatic amino acids (His, Phe, Trp, and Tyr) were determined using spectrophotometric assays that detects the

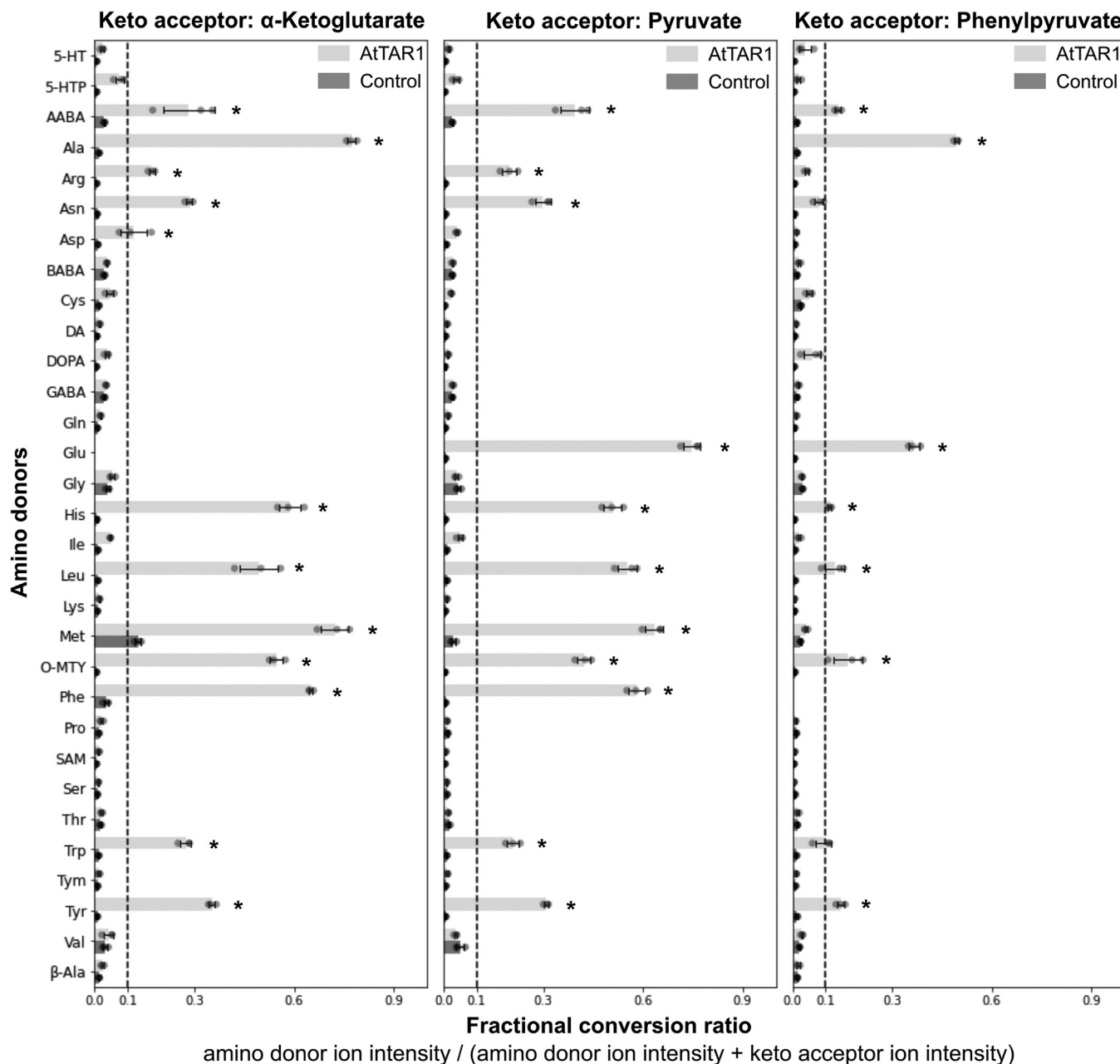


Figure 3. Screening of *AtTAR1* against 31 amino donors and three keto acceptors. Aminotransferase activity of *AtTAR1* was analyzed for 31 amino donors using three keto acceptors, α -ketoglutarate, pyruvate, and phenylpyruvate. Bar chart shows the fractional conversion ratios for each amino donor with *AtTAR1* or the control (no amino donor) \pm the standard deviations for three biological replicates. Individual biological replicates are plotted as closed circles. Dotted line indicates a fractional conversion ratio of 0.1. * indicates a fractional conversion ratio of >0.1 and greater than 10 standard deviations compared to the control. 5-HT, serotonin; 5-HTP, 5-hydroxy-L-tryptophan; AABA, 2-aminobutyric acid; Ala, alanine; Arg, arginine; Asn, asparagine; Asp, aspartic acid; *AtTAT1*, *Arabidopsis thaliana* tyrosine aminotransferase 1; *AtTAR1*, *Arabidopsis thaliana* tryptophan aminotransferase related protein 1; BABA, β -Aminobutyric acid; Cys, cysteine; DA, dopamine; DOPA, L-DOPA; GABA, γ -Aminobutyric acid; Gln, glutamine; Glu, glutamic acid; Gly, glycine; His, histidine; Ile, isoleucine; Leu, leucine; Lys, lysine; Met, methionine; O-MTY, O-methyl-Tyrosine; Phe, phenylalanine; Pro, proline; SAM, S-Adenosyl methionine; Ser, serine; Thr, threonine; Trp, tryptophan; Tym, tyramine; Tyr, tyrosine; Val, valine; β -Ala, β -Alanine.

Mass spectrometry-based screening of aminotransferase

formation of the analogous aromatic keto acids (Fig. 4A) (14). Both *AtTAA1* and *AtTAR1* had the highest catalytic efficiency (k_{cat}/K_m) with Trp, followed by Tyr, Phe, and His. *AtTAR1* had higher k_{cat}/K_m with all substrates than *AtTAA1*, mainly due to its lower K_m toward aromatic amino acids (Fig. 4A). Since AT-catalyzed reactions are typically reversible and with their

amino donor and keto acceptor specificities expected to be similar, the keto acceptor specificity of *AtTAA1* and *AtTAR1* was analyzed to confirm oxime-MSI assay hits. Here, a spectrophotometric tryptophan AT assay using the Salkowski reagent was used to detect IPA generated from Trp by these two tryptophan ATs in the presence of various keto acceptor

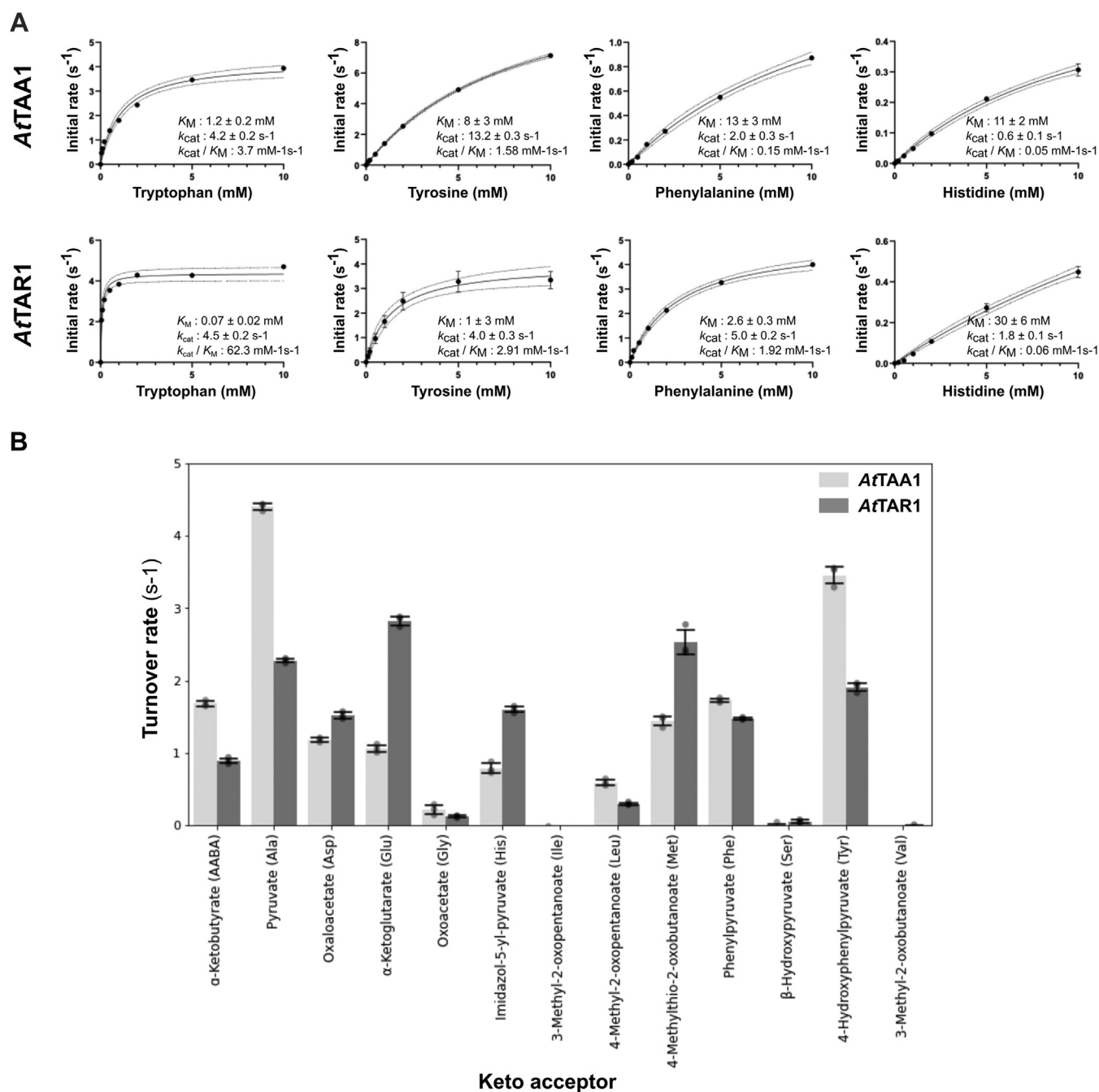


Figure 4. Kinetic parameters and keto acid specificity screening of *AtTAA1* and *AtTAR1*. A, kinetic properties of *AtTAA1* and *AtTAR1* with aromatic amino acid donors. *AtTAA1* and *AtTAR1* (1–10 ng/μl) were incubated with 20 mM keto acid (pyruvate or α-ketoglutarate) and varied concentrations of aromatic amino acids, when their activity increased linearly. Michaelis–Menten equation was fitted using non-linear regression for the calculation of kinetic parameters. Each data point is an average of three separate assays (n = 3). Error bars show SEM. B, tryptophan aminotransferase activity of *AtTAA1* and *AtTAR1* with 13 keto acceptors. X-axis shows the turnover rate of each enzyme with 40 mM tryptophan and 6 mM of keto acid given on the y-axis. Each bar is an average of three biological replicates (n = 3) and the error bar shows the standard deviation. Individual biological replicates are plotted as closed circles. Amino acids given in parentheses show the product formed by the transamination of the keto acid. AABA, 2-aminobutyric acid; Ala, Alanine; Asp, Aspartic acid; *AtTAA1*, *Arabidopsis thaliana* tryptophan aminotransferase of *Arabidopsis* 1; *AtTAR1*, *Arabidopsis thaliana* tryptophan aminotransferase related protein 1; Glu, glutamic acid; Gly, glycine; His, histidine; Ile, isoleucine; Leu, leucine; Met, methionine; Phe, phenylalanine; Ser, serine; Trp, tryptophan; Val, valine.

substrates (14, 17). This assay showed that both *AtTAA1* and *AtTAR1* can use pyruvate, α -ketoglutarate, 4-methylthio-2-oxobutanoate, phenylpyruvate, imidazol-5-yl-pyruvate, 4-hydroxyphenylpyruvate, oxaloacetate, 4-methyl-2-oxopentanoate, and α -ketobutyrate (Fig. 4B). These keto acid substrates correspond to Ala, Glu, Met, Phe, His, Tyr, Asp, Leu, and AABA, respectively, which were detected by the oxime-MSI AT assay in the reverse reactions (Fig. 3). Therefore, three independent assays, including enzyme kinetic analysis, showed consistent results and revealed that TAA1 and TAR1 have similar specificities to amino acids and their corresponding keto acids.

Discussion

The oxime-MSI AT assay enables the detection of transaminated substrates from AT reactions in a high-throughput manner using a MS-based readout without the need of chromatographic separation. Similar to other AT assays, reactions can be carried out using native amino donors and keto acceptors but without the need of a coupled assay or relying on the intrinsic absorbance or fluorescence, which are specific to individual amino donors or keto acceptors (e.g., those containing aromatic groups). As the detection relies on the tagging of the oxime probe to a ketone, the assay can detect all AT reactions that result in the formation of ketone from an amino donor, even beyond amino acids. Therefore, potential AT activity against target molecules relevant to the pharmaceutical and fine chemical industries, like valuable amine drug intermediates, can be screened (35, 36). Also, the oxime probe transfers favorable mass spectrometry properties to the reaction product, increasing the assay sensitivity. We assumed that the coupling efficiency of the oxime probe to all deaminated amino donors is equal as this was shown for other ketone/aldehyde substrates in a previous study (28). The only requirement for the transamination reaction is the formation of a stable ketone. If a reaction product is unstable or highly reactive and loses its ketone group, it cannot be derivatized. For example, the product of glutamine transamination is α -ketoglutaramate that reversibly cyclizes to a lactam (2-hydroxy-5-oxoproline), leaving only $\sim 0.3\%$ present in the open-chain conformation at physiological pH (37). Only the open-chain form of α -ketoglutaramate can be tagged and thus detected.

Furthermore, we showed that the oxime-MSI AT assay can detect AT activity in a semi-quantitative manner allowing for relative quantification, as lowering of the Tyr concentration resulted in proportionally lower fractional conversion ratios of Tyr into hydroxyphenylpyruvate (Fig. 2C). For absolute quantification of the reaction, the use of an internal standard is required. This can be achieved by spiking in a ketone or aldehyde at a fixed concentration during oxime tagging, the ratio of the mass spectral intensity of tagged transaminated amino donor relative to the spiked in ketone/aldehyde can be used to determine the concentration of transaminated amino donor. The internal standard has to have a different mass than the expected transaminated amino donors or the keto acceptor

and preferably has the same or a similar chemical structure (e.g., stable isotope-labeled compounds) to minimize differences in tagging and desorption/ionization efficiencies. However, absolute quantification of selected AT activities, detected from the oxime AT screening, can be easily carried out by other conventional methods, which will provide additional validation, as we demonstrated here (Fig. 4).

We envision that the oxime-MSI AT assay will be used as an HTS platform to identify AT activity with enzyme, amino donor, and keto acceptor combinations, and that 'hits' are validated and characterized in depth by traditional AT activity assays, such as LC/MS or spectroscopy-based methods.

Besides NIMS, other MSI techniques can be used in combination with the oxime-MSI AT assay. The activity of *AtTAT1* with Tyr and α -KG was analyzed using MALDI (Fig. S2). Although NIMS has its advantages over MALDI, including the lack of the requisite addition of matrix and crystal formation and the absence of matrix ions obscuring or interfering with analysis, we understand that MALDI is the most widely used MSI technique, and this shows that the oxime-MSI AT assay is compatible with MALDI analysis (26).

For determining AT activity, we set an arbitrary threshold for fractional conversion rates at >0.1 and it had to be more than 10 standard deviations above the no amino donor control. A fractional conversion rate of 0.1 indicates that the tagged AT reaction product had at least a signal intensity of 10% compared to all oxime-tagged reaction products and keto acceptor. This ensures that the peak of the tagged reaction product ion has a good signal-to-noise ratio. By setting the threshold of 10 standard deviations above the no amino donor control, it ensures that the reaction product was the result of transamination and not background activity or contamination. If the applied threshold is too high, it could produce false negatives. However, lowering the threshold to >0.05 only yields activity with four additional amino donors in combination with all three keto acids and the three ATs, indicating that the threshold is not too strict. For amino acids whose keto acids are commercially available, we confirmed the activities of both *AtTAA1* and *AtTAR1* observed in the oxime-MSI AT assay using a spectrophotometric-based AT assay, indicating that no false positives were observed.

HTS is achieved using acoustic sample deposition and the subsequent analysis by MSI. Here, we arrayed reactions onto a NIMS surface, but other desorption-based MS techniques can be used, including nanospray desorption electrospray ionization and desorption/ionization on silicon (26, 38). Up to 10,000 samples can be spotted onto a NIMS surface and can be analyzed in about 13 h, yielding a sample throughput of 5 s per sample (38). This is a far greater throughput than conventional separation-based MS platforms, such as LC/MS (38). Furthermore, acoustic sample deposition allows for using low reaction volumes and multi-well microplates which reduces costs and makes the assay amenable for automated liquid handling. Overall, the oxime-MSI AT assay can operate at the scale and throughput that is needed to investigate the large number of AT gene candidates and fully characterize the broad substrate specificity/promiscuity of ATs.

Mass spectrometry-based screening of aminotransferase

The oxime-MSI AT assay carried out in this study confirmed that *AtTAR1* has a similar amino donor specificity and keto acceptor preferences as *AtTAA1* (Figs. 3 and S3). This is not surprising, as TAR1 and TAA1 are phylogenetically related proteins, and prior genetic studies suggested that both function in the auxin biosynthetic pathway *via* indole-3-pyruvic acid (34, 39). Both ATs had a preference for α -ketoglutarate and pyruvate as keto acceptors (Figs. 3, 4 and S3). *AtTAR1* was able to use more diverse amino donors than *AtTAA1*—13 vs 11 amino donors, respectively. The exception is Asp, which was only used by *AtTAR1* as an amino donor in combination with α -ketoglutarate as a keto acceptor. Both *AtTAT1* and *AtTAR1* can use Trp as an amino donor and showed activity above the initial threshold with Trp (Figs. 3 and S4). Lowering of the detection threshold would also confirm the usage of Trp by *AtTAA1* (Fig. S3), a known amino donor for *AtTAA1* (33). A prior study showed that TAA1 is feedback-inhibited by the transaminated product of Trp, indole-3-pyruvate, which could explain the low fractional conversion rate for Trp by TAA1 and not for TAT1 or TAR1 (40).

Enzyme kinetic analysis further validated that *AtTAA1* and *AtTAR1* are *bona fide* tryptophan ATs, since both enzymes showed significantly higher catalytic efficiency with Trp compared to other aromatic amino acids (Fig. 4A). Interestingly, however, *AtTAR1* had an ~ 17 fold higher catalytic efficiency than *AtTAA1*, mainly because of its much lower K_m with Trp, suggesting that TAR1 can function at much lower Trp concentrations than *AtTAA1* *in planta*. AABA and O-MTY were identified as novel substrates for all three ATs (Figs. 3, S3 and S4). AABA has a similar structure to that as Ala, and other ATs that were able to use Leu, Ala, Met, and Phe are also able to use AABA as an amino donor (41). This finding also demonstrates that the easily scalable nature of the oxime MS assay enables detection of novel AT activity and also provides rich experimental data to facilitate structure–function analyses of the AT enzyme family.

Our analyses of the keto acid specificity by spectrophotometric assays showed similar substrate preferences between amino acids and their corresponding keto acids for *AtTAA1* and *AtTAR1* (Figs. 3 and 4). For example, Glu, Ala, Met, His, Tyr, Phe, and Leu act as amino donors, and their corresponding keto acids, α -ketoglutarate, pyruvate, 4-methylthio-2-oxobutanoate, imidazol-5-yl-pyruvate, 4-hydroxyphenylpyruvate, phenylpyruvate, and 4-methyl-2-oxopentanoate act as keto acceptors. Therefore, the amino donor substrate specificity determined by the oxime-MSI assay for a certain AT will likely reflect its keto acid substrate specificity. In contrast to *AtTAA1* that clearly prefers pyruvate and 4-hydroxyphenylpyruvate as keto acceptors, *AtTAR1* showed a broader keto acid specificity with similar preferences to pyruvate, α -ketoglutarate, 4-methylthio-2-oxobutanoate, 4-hydroxyphenylpyruvate, oxaloacetate, phenylpyruvate, imidazole-5-yl-pyruvate (Fig. 4). However, the physiological functions of *AtTAR1*'s broad keto acid specificity remain to be investigated *in vivo*. Interestingly, the activity of *AtTAA1* and *AtTAR1* with pyruvate and α -ketobutyrate showed a similar pattern; TAA1 showing roughly double the activity of

AtTAR1 with both substrates (Fig. 4). Considering pyruvate and α -ketobutyrate are similar in their structure, substrate specificity screenings can potentially be used to predict AT activity with structurally similar compounds (33, 40).

In conclusion, here we established the oxime-MSI AT assay and demonstrated its suitability for HTS of AT amino donor and keto acceptor specificity. This new technology enabled screening of substrate specificity and revealed that *AtTAR1* can use 13 amino acids as donors. In future studies, these properties could be used to build enzyme structure–function models, where experimental data gathered on representative AT enzymes is used to predict substrate specificities of unknown ATs based on phylogenetic relatedness, AT sequence and structure, and chemical properties of the substrates. Thus, this novel technology unlocks an exciting opportunity to expand our knowledge of AT characteristics and functions in N metabolic networks through comprehensive determination of AT substrate specificity.

Experimental procedures

All individual chemicals were purchased from Sigma Aldrich except for SAM (New England Biolabs). Water (Honeywell International Inc), acetonitrile (OmniSolv, Sigma Aldrich), and methanol (J.T.Baker) were of LC-MS grade.

Cloning of plasmid(s) for recombinant expression of ATs

The same pET28a expression construct described in Wang *et al.* (2016) was used for *A. thaliana* TyrAT 1 (TAT1, At5g53970). The entire coding sequence of tryptophan AT of Arabidopsis 1 (TAA1, AT1G70560) and tryptophan AT-related 1 (TAR1, AT1G23320) were synthesized by Synbio Technologies and cloned into the pET28a vector (Novagen) between the NdeI and BamHI sites.

Recombinant production of ATs

Chemical competent Rosetta-2 (DE3) *Escherichia coli* cells (Novagen) were transformed with the pET28a vector expressing TAT1, TAA1, or TAR1 and selected on LB agar with 50 μ g/ml kanamycin. Colonies for each construct were picked, inoculated in 10 ml LB medium with 50 μ g/ml kanamycin, and incubated overnight at 37 °C, 200 rpm. 10 milliliters of the culture was transferred to 500 ml of fresh LB medium and grown at 37 °C, 200 rpm until A600 reached ~ 0.6 , when the temperature was dropped to 22 °C and Iso-propyl β -D-1-thiogalactopyranoside was added at 0.2 mM final concentration. After overnight incubation at 30 °C, 200 rpm, cells were harvested by centrifugation at 6000 rpm for 20 min at 4 °C. The pellet was either stored at -80 °C for later use, or resuspended in 10 ml of lysis buffer containing 50 mM sodium phosphate (pH 8.0), 300 mM NaCl, 25 μ M PLP, and 0.25 mg/ml lysozyme (Sigma Aldrich). After disrupting cells by three freeze-thaw cycles and sonication, the soluble extract was obtained by centrifugation at 4 °C, 18,000g for 30 min. His-tagged recombinant proteins were purified using a nickel-conjugated HisTrap Fastflow crude column (Cytiva) with

ÄKTA pure chromatography system (Cytiva). Purified proteins were desalted with Sephadex G-50 superfine resin (Cytiva) into 100 mM HEPES buffer (pH 7.5) containing 25 μ M PLP and 10% glycerol. Recombinant proteins were separated by SDS-PAGE, and the gels were stained by Coomassie Blue, imaged by ChemiDoc (Bio-Rad Laboratories, Inc), and their purity was assessed by ImageJ (<https://imagej.net/ij/index.html>) (Fig. S1).

AT amino donor screening

All amino donor substrates were initially dissolved in 0.25 N NaOH at 100 mM, as the solubility of Tyrin water is low (<2 mM) (42). High-throughput AT reactions were tested in a reaction mixture with a final concentration of 100 mM Hepes pH 7.4, 10 mM amino donor, 6 mM keto acceptor, 0.5 mM PLP, and 20 to 40 ng/ μ l enzyme (0.3–5.12 ng/ μ l enzyme for kinetic studies), with a final pH of 7.6 to 8.0, which is around the optimum of *AtTAT1* and is similar to other plant aromatic amino acid AT activities and enzymes (15). Reactions were performed in 384-well plates with a final reaction volume of 2.5 μ l. The reaction mixtures were incubated at 30 °C for 60 min and directly followed by oxime tagging.

AT activity analysis by oxime tagging and NIMS or MALDI mass spectrometry

Transaminated amino donor substrates and nondepleted keto acid acceptor substrates were analyzed using oxime bioconjugate chemistry and NIMS. The synthesis and the subsequent oxime derivatization reactions with the O-alkyloxyamine fluoros tag (m/z 793.2365) were carried out as reported previously (28). Enzymatic reactions were diluted 1:5 using H₂O. A 1 μ l aliquot of the diluted enzymatic reactions was transferred into a 384 well plate containing 6 μ l of 100 mM glycine acetate (pH 1.3), 3 μ l of ethanol, 1 μ l of O-alkyloxyamine fluoros tag [10 mM in 1:1 (v/v) water:methanol], and 0.26 μ l of aniline per well. The mixture was incubated at room temperature (RT) for 16 h before NIMS or MALDI analysis.

For NIMS analysis, oxime reactions were prepared for either acoustic sample deposition or manual spotting onto a NIMS substrate which was processed as described previously (24). For each sample, 1 μ l of the oxime reaction mixture, 5 μ l water, 2 μ l methanol, and 0.02 μ l formic acid were combined. For acoustic sample deposition, samples were printed onto the NIMS surface using an ATS-100 acoustic transfer system (BioSera) with a sample deposition volume of 10 nl. Samples were printed in clusters of three biological replicates, with the microarray spot pitch (center-to-center distance) set at 900 μ m. For manual spotting, samples (0.5 μ l) were manually spotted onto the NIMS surface with three biological replicates.

For MALDI analysis, the oxime reaction mixture was mixed 1:1 with the matrix α -cyano-4-hydroxycinnamic acid (10 mg/ml in MeOH + 0.5% FA). Samples (0.8 μ l) were manually spotted onto a stainless steel MALDI target plate with three biological replicates.

MS-based imaging was performed using a 5800 MALDI TOF/TOF (AB Sciex) mass spectrometer with laser intensity of

3000 to 4200 over a mass range of 500 – 2000 Da. Each position accumulated 20 laser shots. The instrument was controlled using the MALDI-MSI 4800 Imaging Tool using a 75 μ m step size. Average ion intensity of the conjugated transaminated amino donor and keto acceptors substrates were determined using the OpenMSI Arrayed Analysis Toolkit (OMAAAT) software package (31). MSI data obtained in this study is available and browsable at OpenMSI (43).

Enzyme kinetic assays

Enzyme kinetic assays of *AtTAA1* and *AtTAR1* were conducted as described previously (14). Briefly, the assays were carried out in a reaction mixture containing 100 mM HEPES pH 8.0, 20 mM keto acceptor pyruvate (for *AtTAA1* with Trp, Tyr, and Phe) or α -ketoglutarate (for *AtTAA1* with His and *AtTAR1* with Trp, Tyr, Phe, and His), 0.2 mM PLP, 1 to 10 ng/ μ l enzyme, and 0 to 10 mM final concentrations of amino acid donors. The reactions were initiated by the addition of the amino acid donor to the reaction mixture and incubated at 30 °C for five or 10 min, depending on the enzymatic rate, to achieve conditions where the product formation linearly increased with time and enzyme concentrations. Reactions with Trp, Tyr, and Phe were terminated by adding sodium hydroxide (final 0.4 M), and the reaction with His was terminated by boiling the reaction mixture for 10 min. Reactions with His were terminated by adding 1 \times volume of 1 M borate buffer pH 8.5, and cooled down to RT. Formation of phenylpyruvate, 4-hydroxyphenylpyruvate, indole-3-pyruvate, and imidazol-5-yl-pyruvate were detected by measuring the absorbance at 320, 331, 334, and 293 nm, respectively. Absorbance values were converted to concentration using standard curves of the corresponding keto acids. Kinetic parameters were calculated from the average of three separate assays by fitting the Michaelis–Menten equation using nonlinear regression function of GraphPad (<https://www.graphpad.com/scientific-software/prism/>).

AT keto acceptor screening

Reverse reactions of tryptophan AT, *i.e.*, production of amino acids, were tested in a reaction mixture with a final concentration of 100 mM phosphate buffer pH 8.0, 40 mM tryptophan, 0.025 mM PLP, 1 ng/ μ l enzyme, and 6 mM of the keto acceptor given on the figure, in 300 μ l final reaction volume. Reactions were initiated by the addition of tryptophan to the remaining components. The reaction mixtures were incubated at 30 °C for 5 min and terminated by the addition of 2 \times volume of Salkowski reagent (10 mM FeCl₃ and 35% [v/v] H₂SO₄). After incubating at RT for 10 min in the dark, the formation of the pink/purple product was measured spectrophotometrically at λ 530 nm using the Infinite M Plex plate reader (Tecan Group Ltd). The reaction without any keto acid acceptor was used as the background control. Kinetic parameters were calculated with GraphPad. All enzyme assays were performed under the condition where the product formation increased proportionally to the enzyme concentration and the reaction time.

Mass spectrometry-based screening of aminotransferase

Data availability

All MSI ion intensity data for the bioconjugates obtained using the OMAAT algorithm can be found in Table S1. The OMAAT Python code and Jupyter notebooks are available at GitHub: <https://github.com/biorack/omaat>.

Raw MSI data can be found and is browsable at OpenMSI: <http://openmsi.nersc.gov>. TAT NIMS MSI dataset:

20210330MdR_5800_NIMS_AT_screen_TAT.h5 (

TAA NIMS MSI dataset: 20210402MdR_5800_NIMS_AT_screen_TAA1.h5 (

TAR NIMS MSI dataset: 20210401MdR_5800_NIMS_AT_screen_TAR1.h5 (

Supporting information—This article contains supporting information.

Acknowledgments—This work was supported by the U.S. Department of Energy, Office of Science, Office of Biological and Environmental Research, Genomic Science Program grant no. DE-SC0020390 and the Joint Genome Institute award no. CSP-503757. The Department of Energy Joint BioEnergy Institute is supported by the US Department of Energy, Office of Science, Office of Biological and Environmental Research, through contract DE-AC02-05CH11231.

Author contributions—M. D. R. and T. R. N. conceptualization; M. D. R., K. K., K. D., H. A. M., and T. R. N. methodology; M. D. R. and B. P. B. software; M. D. R. and K. K. validation; M. D. R., K. K., and B. P. B. formal analysis; H. A. M. and T. R. N. supervision; H. A. M. and T. R. N. funding acquisition; M. D. R. writing – original draft; K. K., H. A. M., and T. R. N. writing – review and editing.

Conflict of interest—The authors declare that they have no conflict of interest with the contents of this article.

Abbreviations—The abbreviations used are: AABA, 2-aminobutyric acid; Ala, alanine; Arg, arginine; Asn, asparagine; Asp, aspartic acid; AT, Aminotransferase; AtTAA1, *Arabidopsis thaliana* tryptophan aminotransferase of *Arabidopsis* 1; AtTAR1, *Arabidopsis thaliana* tryptophan aminotransferase related protein 1; AtTAT1, *Arabidopsis thaliana* tyrosine aminotransferase 1; Glu, glutamic acid; His, histidine; HTS, high-throughput screening; IPA, indole-3-pyruvic acid; Leu, leucine; Met, methionine; MSI, mass spectrometry imaging; NIMS, nanostructure-initiator mass spectrometry; O-MTY, O-methyl-tyrosine; PLP, Pyridoxal 5'-phosphate; Phe, phenylalanine; Trp, tryptophan; Tyr, tyrosine; α -KG, α -ketoglutarate.

References

1. Toney, M. D. (2014) Aspartate aminotransferase: an old dog teaches new tricks. *Arch. Biochem. Biophys.* **544**, 119–127
2. Koper, K., Han, S.-W., Pastor, D. C., Yoshikuni, Y., and Maeda, H. A. (2022) Evolutionary origin and functional diversification of aminotransferases. *J. Biol. Chem.* **298**, 102122
3. Percudani, R., and Peracchi, A. (2009) The B6 database: a tool for the description and classification of vitamin B6-dependent enzymatic activities and of the corresponding protein families. *BMC Bioinformatics* **10**, 273
4. Percudani, R., and Peracchi, A. (2003) A genomic overview of pyridoxal-phosphate-dependent enzymes. *EMBO Rep.* **4**, 850–854
5. Felig, P., Pozefsky, T., Marliss, E., and Cahill, G. F., Jr. (1970) Alanine: key role in gluconeogenesis. *Science* **167**, 1003–1004
6. Hwang, B.-Y., Lee, H.-J., Yang, Y.-H., Joo, H.-S., and Kim, B.-G. (2004) Characterization and investigation of substrate specificity of the sugar aminotransferase WecE from *E. coli* K12. *Chem. Biol.* **11**, 915–925
7. Zheng, Z., Guo, Y., Novák, O., Dai, X., Zhao, Y., Ljung, K., et al. (2013) Coordination of auxin and ethylene biosynthesis by the aminotransferase VAS1. *Nat. Chem. Biol.* **9**, 244–246
8. Huß, S., Judd, R. S., Koper, K., Maeda, H. A., and Nikoloski, Z. (2022) An automated workflow that generates atom mappings for large-scale metabolic models and its application to *Arabidopsis thaliana*. *Plant J.* **111**, 1486–1500
9. Bailey-Serres, J., Parker, J. E., Ainsworth, E. A., Oldroyd, G. E. D., and Schroeder, J. I. (2019) Genetic strategies for improving crop yields. *Nature* **575**, 109–118
10. Chubukov, V., Gerosa, L., Kochanowski, K., and Sauer, U. (2014) Coordination of microbial metabolism. *Nat. Rev. Microbiol.* **12**, 327–340
11. Lukey, M. J., Katt, W. P., and Cerione, R. A. (2017) Targeting amino acid metabolism for cancer therapy. *Drug Discov. Today* **22**, 796–804
12. Urrestarazu, A., Vissers, S., Iraqui, I., and Gresson, M. (1998) Phenylalanine- and tyrosine-auxotrophic mutants of *Saccharomyces cerevisiae* impaired in transamination. *Mol. Gen. Genet.* **257**, 230–237
13. Pinto, J. T., Krasnikov, B. F., Alcutt, S., Jones, M. E., Dorai, T., Villar, M. T., et al. (2014) Kynurenine aminotransferase III and glutamine transaminase L are identical enzymes that have cysteine S-conjugate β -lyase activity and can transaminate L-selenomethionine. *J. Biol. Chem.* **289**, 30950–30961
14. Koper, K., Hataya, S., Hall, A. G., Takasuka, T. E., and Maeda, H. A. (2022) Biochemical characterization of plant aromatic aminotransferases. In *Methods in Enzymology*. Academic Press, Cambridge, MA
15. Wang, M., Toda, K., and Maeda, H. A. (2016) Biochemical properties and subcellular localization of tyrosine aminotransferases in *Arabidopsis thaliana*. *Phytochemistry* **132**, 16–25
16. Schätzle, S., Höhne, M., Redestad, E., Robins, K., and Bornscheuer, U. T. (2009) Rapid and sensitive kinetic assay for characterization of ω -transaminases. *Anal. Chem.* **81**, 8244–8248
17. Szkop, M., Sikora, P., and Orzechowski, S. (2012) A novel, simple, and sensitive colorimetric method to determine aromatic amino acid aminotransferase activity using the Salkowski reagent. *Folia Microbiol.* **57**, 1–4

18. Truppo, M. D., Rozzell, J. D., Moore, J. C., and Turner, N. J. (2009) Rapid screening and scale-up of transaminase catalysed reactions. *Org. Biomol. Chem.* **7**, 395–398
19. Hopwood, J., Truppo, M. D., Turner, N. J., and Lloyd, R. C. (2011) A fast and sensitive assay for measuring the activity and enantioselectivity of transaminases. *Chem. Commun.* **47**, 773–775
20. Baud, D., Ladkau, N., Moody, T. S., Ward, J. M., and Hailes, H. C. (2015) A rapid, sensitive colorimetric assay for the high-throughput screening of transaminases in liquid or solid-phase. *Chem. Commun.* **51**, 17225–17228
21. Schätzle, S., Höhne, M., Robins, K., and Bornscheuer, U. T. (2010) Conductometric method for the rapid characterization of the substrate specificity of amine-transaminases. *Anal. Chem.* **82**, 2082–2086
22. Mathew, S., Shin, G., Shon, M., and Yun, H. (2013) High throughput screening methods for ω -transaminases. *Biotechnol. Bioproc. Eng.* **18**, 1–7
23. Northen, T. R., Lee, J.-C., Hoang, L., Raymond, J., Hwang, D.-R., Yannone, S. M., *et al.* (2008) A nanostructure-initiator mass spectrometry-based enzyme activity assay. *Proc. Natl. Acad. Sci. U. S. A.* **105**, 3678–3683
24. Northen, T. R., Yanes, O., Northen, M. T., Marrinucci, D., Uritboonthai, W., Apon, J., *et al.* (2007) Clathrate nanostructures for mass spectrometry. *Nature* **449**, 1033–1036
25. Heins, R. A., Cheng, X., Nath, S., Deng, K., Bowen, B. P., Chivian, D. C., *et al.* (2014) Phylogenomically guided identification of industrially relevant GH1 β -glucosidases through DNA synthesis and nanostructure-initiator mass spectrometry. *ACS Chem. Biol.* **9**, 2082–2091
26. de Rond, T., Danielewicz, M., and Northen, T. (2014) High throughput screening of enzyme activity with mass spectrometry imaging. *Curr. Opin. Biotechnol.* **31C**, 1–9
27. de Rond, T., Gao, J., Zargar, A., de Raad, M., Cunha, J., Northen, T. R., *et al.* (2019) A high-throughput mass spectrometric enzyme activity assay enabling the discovery of cytochrome P450 biocatalysts. *Angew. Chem. Weinheim Bergstr. Ger.* **131**, 10220–10225
28. Deng, K., Takasuka, T. E., Heins, R., Cheng, X., Bergeman, L. F., Shi, J., *et al.* (2014) Rapid kinetic characterization of glycosyl hydrolases based on oxime derivatization and nanostructure-initiator mass spectrometry (NIMS). *ACS Chem. Biol.* **9**, 1470–1479
29. Deng, K., George, K. W., Reindl, W., Keasling, J. D., Adams, P. D., Lee, T. S., *et al.* (2012) Encoding substrates with mass tags to resolve stereospecific reactions using nimzyme. *Rapid Commun. Mass Spectrom.* **26**, 611–615
30. Greving, M., Cheng, X., Reindl, W., Bowen, B., Deng, K., Louie, K., *et al.* (2012) Acoustic deposition with NIMS as a high-throughput enzyme activity assay. *Anal. Bioanal. Chem.* **403**, 707–711
31. de Raad, M., de Rond, T., Rübél, O., Keasling, J. D., Northen, T. R., and Bowen, B. P. (2017) OpenMSI arrayed analysis toolkit: analyzing spatially defined samples using mass spectrometry imaging. *Anal. Chem.* **89**, 5818–5823
32. Zhang, J. H., Chung, T. D., and Oldenburg, K. R. (1999) A simple statistical parameter for use in evaluation and validation of high throughput screening assays. *J. Biomol. Screen.* **4**, 67–73
33. Tao, Y., Ferrer, J.-L., Ljung, K., Pojer, F., Hong, F., Long, J. A., *et al.* (2008) Rapid synthesis of auxin via a new tryptophan-dependent pathway is required for shade avoidance in plants. *Cell* **133**, 164–176
34. Wang, Q., Qin, G., Cao, M., Chen, R., He, Y., Yang, L., *et al.* (2020) A phosphorylation-based switch controls TAA1-mediated auxin biosynthesis in plants. *Nat. Commun.* **11**, 679
35. Kelly, S. A., Pohle, S., Wharry, S., Mix, S., Allen, C. C. R., Moody, T. S., *et al.* (2018) Application of ω -transaminases in the pharmaceutical industry. *Chem. Rev.* **118**, 349–367
36. Kelly, S. A., Mix, S., Moody, T. S., and Gilmore, B. F. (2020) Transaminases for industrial biocatalysis: novel enzyme discovery. *Appl. Microbiol. Biotechnol.* **104**, 4781–4794
37. Cooper, A. J. L., and Kuhara, T. (2014) α -Ketoglutaramate: an overlooked metabolite of glutamine and a biomarker for hepatic encephalopathy and inborn errors of the urea cycle. *Metab. Brain Dis.* **29**, 991–1006
38. de Raad, M., Fischer, C. R., and Northen, T. R. (2016) High-throughput platforms for metabolomics. *Curr. Opin. Chem. Biol.* **30**, 7–13
39. Won, C., Shen, X., Mashiguchi, K., Zheng, Z., Dai, X., Cheng, Y., *et al.* (2011) Conversion of tryptophan to indole-3-acetic acid by tryptophan aminotransferases of Arabidopsis and Yuccas in Arabidopsis. *Proc. Natl. Acad. Sci. U. S. A.* **108**, 18518–18523
40. Sato, A., Soeno, K., Kikuchi, R., Narukawa-Nara, M., Yamazaki, C., Kakei, Y., *et al.* (2022) Indole-3-pyruvic acid regulates TAA1 activity, which plays a key role in coordinating the two steps of auxin biosynthesis. *Proc. Natl. Acad. Sci. U. S. A.* **119**, e2203633119
41. Wenger, A., Schmidt, R. S., Portmann, R., Roetschi, A., Eugster, E., Weiskopf, L., *et al.* (2020) Identification of a species-specific aminotransferase in *pediococcus acidilactici* capable of forming α -aminobutyrate. *AMB Express* **10**, 100
42. Hitchcock, D. I. (1924) The solubility of tyrosine in acid and in alkali. *J. Gen. Physiol.* **6**, 747–757
43. Rübél, O., Greiner, A., Cholia, S., Louie, K., Bethel, E. W., Northen, T. R., *et al.* (2013) OpenMSI: a high-performance web-based platform for mass spectrometry imaging. *Anal. Chem.* **85**, 10354–10361